Structural and Proteomic Changes in Viable but Non-culturable Vibrio cholerae

Susanne Brenzinger, Lizah T. van Der Aart, Gilles P. van Wezel, Jean-Marie Lacroix, Timo Glatter, Ariane Briegel

frontiers in Microbiology

ORIGINAL RESEARCH
published: 17 April 2019
doi: 10.3389/fmicb.2019.00793

Structural and Proteomic Changes in Viable but Non-culturable *Vibrio cholerae*

Susanne Brenzinger[1], Lizah T. van der Aart[1], Gilles P. van Wezel[1], Jean-Marie Lacroix[2], Timo Glatter[3] and Ariane Briegel[1]**

[1] Department of Microbial Biotechnology & Health, Institute of Biology Leiden, Leiden University, Leiden, Netherlands, [2] Unité de Glycobiologie Structurale et Fonctionnelle, UMR CNRS 8576, Université de Lille Sciences et Technologies, Villeneuve d'Ascq, France, [3] Facility for Bacterial Proteomics and Mass Spectrometry, Max-Planck Institute for Terrestrial Microbiology, Marburg, Germany

Aquatic environments are reservoirs of the human pathogen *Vibrio cholerae* O1, which causes the acute diarrheal disease cholera. Upon low temperature or limited nutrient availability, the cells enter a viable but non-culturable (VBNC) state. Characteristic of this state are an altered morphology, low metabolic activity, and lack of growth under standard laboratory conditions. Here, for the first time, the cellular ultrastructure of *V. cholerae* VBNC cells raised in natural waters was investigated using electron cryo-tomography. This was complemented by a comparison of the proteomes and the peptidoglycan composition of *V. cholerae* from LB overnight cultures and VBNC cells. The extensive remodeling of the VBNC cells was most obvious in the passive dehiscence of the cell envelope, resulting in improper embedment of flagella and pili. Only minor changes of the peptidoglycan and osmoregulated periplasmic glucans were observed. Active changes in VBNC cells included the production of cluster I chemosensory arrays and change of abundance of cluster II array proteins. Components involved in iron acquisition and storage, peptide import and arginine biosynthesis were overrepresented in VBNC cells, while enzymes of the central carbon metabolism were found at lower levels. Finally, several pathogenicity factors of *V. cholerae* were less abundant in the VBNC state, potentially limiting their infectious potential. This study gives unprecedented insight into the physiology of VBNC cells and the drastically altered presence of their metabolic and structural proteins.

Keywords: *Vibrio cholerae*, viable but non-culturable, proteomics, electron cryotomography, cell envelope, bacterial ultrastructure

OPEN ACCESS

Edited by:
Ivan Mijakovic, Chalmers University of Technology, Sweden

Reviewed by:
Christopher John Grim, United States Food and Drug Administration, United States
Carla Pruzzo, University of Genoa, Italy

****Correspondence:***
Susanne Brenzinger
s.brenzinger@biology.leidenuniv.nl
Ariane Briegel
a.briegel@biology.leidenuniv.nl

Specialty section:
This article was submitted to Microbial Physiology and Metabolism, a section of the journal Frontiers in Microbiology

Received: *15 October 2018*
Accepted: *28 March 2019*
Published: *17 April 2019*

Citation:
Brenzinger S, van der Aart LT, van Wezel GP, Lacroix J-M, Glatter T and Briegel A (2019) Structural and Proteomic Changes in Viable but Non-culturable Vibrio cholerae. Front. Microbiol. 10:793. doi: 10.3389/fmicb.2019.00793

INTRODUCTION

Changes in the physical and chemical properties of their environment, such as heat, cold and salt stress, oxygen and nutrient deprivation, desiccation and changes in osmolarity, threaten the survival of bacteria, and they have therefore evolved various strategies to evade detrimental effects (Merchant and Helmann, 2012; Alvarez-Ordóñez et al., 2015; Guan et al., 2017). The facultative human pathogen *Vibrio cholerae*, is common in brackish and estuarine waters where it is often associated with aquatic flora and fauna (Blake et al., 1977; Huq et al., 1983; Tamplin et al., 1990; Balakrish Nair et al., 1991). Like many other bacteria, *V. cholerae* enters a state of restrained metabolic activity when confronted with cues like low temperatures and or low nutrient availability

over extended periods of time (Xu et al., 1982; Mederma et al., 1992; Rahman et al., 1994; Oliver et al., 1995; Oliver, 2005, 2010; Morishige et al., 2015; Pinto et al., 2015). Once the cells have entered this state, *V. cholerae* does not readily start to grow and reproduce when they are returned to more favorable and nutrient-rich media, and their status has, therefore, been termed "viable but non-culturable" (VBNC) (Xu et al., 1982; Kell et al., 1998; Bergkessel et al., 2016).

Under standard laboratory conditions, *V. cholerae* cells are slightly bent, comma-shaped rods. A characteristic morphological feature of *V. cholerae* VBNC cells is a smaller size and a round, coccoid shape with an increased gap between the cytoplasmic and outer membrane (OM), which was previously observed in transmission electron microscopy (TEM) studies (Chaiyanan et al., 2007; Krebs and Taylor, 2011; Kim et al., 2018). It is currently unknown how this is reflected in altered peptidoglycan architecture, changes in the membrane structures, or the composition of the periplasmic content of *V. cholerae*. An additional limitation lays in the published TEM images themselves, which were generated using fixed, stained and sectioned cells. This technique is known to affect or obscure the delicate ultrastructure of cells (Ayache et al., 2012). For example, *Escherichia coli* VBNC cells that were prepared that way were interpreted as dead, due to their seemingly empty cytosol (Kim et al., 2018). The presence of several macromolecular complexes in VBNC cells was revealed using other techniques. For example, the toxin co-regulated pilus (TCP) and the flagellum were detected in cultures that are transitioning into, or have already entered, the VBNC state using transcription based methods or immunolabeling (Asakura et al., 2007; Krebs and Taylor, 2011; Xu et al., 2018). Unfortunately, these methods can only detect the presence of macromolecular complex components, but whether those machineries are still properly assembled and embedded in the envelope remained unclear. It is also unknown if and how these structural changes are regulated. Several studies have focused on either individual regulatory and structural components involved in VBNC formation, or analyzed the transcriptional profile of VBNC cells [see review (Pinto et al., 2015)]. Unfortunately, the transcriptional studies are difficult to compare with each other as gene targets were not featured in all data sets or the results were contradicting each other (González-Escalona et al., 2006; Asakura et al., 2007; Xu et al., 2018).

To gain detailed insights into the structural makeup of *V. cholerae* VBNC cells, we studied the morphology and structural adaptation of *V. cholerae* VBNC cells using electron cryo-tomography (ECT). The advantage of this method is that the cells can be preserved in a near-native state as the samples are directly applied from the culture to the grid and flash-frozen without staining or dehydration steps. Thus, *V. cholerae* VBNC cells can be visualized in 3D and at macromolecular resolution, resulting in clear and authentic representations of different cellular textures and large macromolecules (Jensen and Briegel, 2007; Oikonomou et al., 2016). This approach was paired with a proteomic analysis of the VBNC cells, as well as a biochemical analysis of the peptidoglycan composition and the presence and abundance of osmoregulated periplasmic glucans. Together, these complementary analysis methods reveal several characteristic changes of the cell morphology and function of VBNC cells.

MATERIALS AND METHODS

Bacterial Strain, Media and VBNC Inducing Conditions

Vibrio cholerae O1 biovar El Tor str. N16961 was used in this study. A small amount of these cells from lysogeny broth (LB) plates was used to inoculate three overnight cultures of 250 ml low salt LB. These cultures were grown at 30°C for 18 h shaking at 200 rpm with a final OD_{600} of 2.5, corresponding to $\sim 2 \cdot 10^9$ CFU. Fifty milliliters of the cells were harvested in 50 ml conical polypropylene tubes using centrifugation (20 min at 5000 × g). Cell pellets were carefully resuspended in cold natural waters, closed and kept at 4°C in the dark on a rocking platform set to low agitation. Total cell numbers were enumerated from the biological triplicates from a dilution series in the respective incubation waters using an improved Neubauer counting chamber. Cells were considered to be in the VBNC state if no CFU were observed in an undiluted volume of 100 µl from any of the three biological triplicates. Samples for electron microscopy or proteomic analysis were taken 30 days after no CFU could be detected.

Natural waters were collected at the following sites: natural fresh water (NFW) at 51°52′50.3″N 5°59′52.2″E, natural brackish water (NBW) containing 13 g chloride/ l was collected at 53°06′02.4″N 4°53′50.5″E and natural salt water (NSW) at 53°06′11.7″N 4°53′54.8″E. All waters were filtered through a series of whatman filters, sterile filtered using a 0.22 µm filter followed by autoclaving. Waters were stored at 4°C until use.

Live/Dead Stain

The fraction of live cells was determined as previously described (Terzieva et al., 1996). In essence 200 µl of a 1:50 dilution of each incubation was mixes with 1 µl of Syto9 and propidium iodide each. The mixture was incubated at room temperature for 20 min in the dark before 3 µl were applied to an agarose slab and imaged on a Zeiss Axioplan 2 equipped with a Zeiss AxioCam MRc 5 digital color camera. At least 500 cells from randomly chosen areas were quantified. Images were processed using ImageJ. Cells with a red, orange, or yellow hue were rated as "dead" and green cells as "live".

Electron Cryo-Tomography

Eighteen µ l of cell suspension from the respective cultures was gently mixed with 2 µl protein A-treated 10 nm colloidal gold solution (Cell Microscopy Core, Utrecht, The Netherlands) by pipetting. Aliquots of 3 µl were applied to a plasma-cleaned R2/2 copper Quantifoil grid (Quantifoil Micro Tools, Jena, Germany). Plunge freezing into liquid ethane was carried out using a Leica EMGP (Leica microsystems, Wetzlar, Germany) set to 1 s blotting inside the chamber set at 20°C and 95% humidity. Grids were stored in liquid nitrogen until imaging.

Data acquisition was performed on a Titan Krios transmission electron microscope (Thermo Fisher Scientific, Hillsboro, OR,

USA) operating at 300 kV. Images were recorded with a Gatan K2 Summit direct electron detector (Gatan, Pleasanton, CA) equipped with a GIF-quantum energy filter (Gatan) operating with a slit width of 20eV. Tomograms were recorded at a nominal magnification of 42,000x (pixel size of 3.513 Å). Using UCSF tomography data collection software (Zheng et al., 2007), all tilt series were collected using a bidirectional tilt scheme which started with 0° to −54° followed by 0° to 54° tilting with a 2° increment. Defocus was set to −8 µm. The cumulative exposure was 120 e-/ Å^2. Drift correction and bead-tracking based tilt series alignment were done using software package IMOD (Kremer et al., 1996). Tomograms were reconstructed using simultaneous iterative reconstruction (SIRT) with iteration number set to 4.

Line scans perpendicular to the OM or sheath membrane was done using IMOD. Twenty nine measurements from five cells each were recorded.

Osmoregulated Periplasmic Glucans (OPG) Analysis

Bacteria (100 mL) were grown in LB with several NaCl concentrations or in various natural waters. Bacteria were collected by centrifugation at 4°C for 15 min at 8,000 g. Cell pellets were suspended in 20 mL of distilled water and lysed with 5% trichloroacetic acid. After centrifugation at 4°C for 30 min at 8,000 g, the supernatant was neutralized with ammonium hydroxide 10% and concentrated by rotary evaporation. The resulting material (2 mL) was fractionated by gel filtration on a Bio-Gel P-4 column (length: 47 cm, diameter: 1.7 cm) equilibrated with 0.5% acetic acid. The column was eluted in the same buffer at a flow rate of 15 mL h-1 and fractions of 1.5 mL were collected. Presence of oligosaccharides in each fraction was determined by the colorimetrically anthrone procedure (Spiro, 1966). Fractions containing OPGs were pooled and total content was determined by the same procedure.

Peptidoglycan Analysis

Murein sacculi were purified as described previously (Cava et al., 2011). In essence, 50 ml cell material of LB overnight cultures or VBNC (NSW) cell suspensions was pelleted, resuspended in 5 ml phosphate buffered saline (PBS) and slowly added to 10 ml of boiling 10% sodium dodecyl sulfate while stirring. Samples were boiled for 4 h, then stirred overnight at 37°C. Cell wall material was then pelleted by ultracentrifugation (85.000 rpm, 0.5 h) and washed in MQ water. Sacculi were digested with pronase E (0.1 mg/ml) in a Tris-HCl 10 mM pH 7.5 buffer for 1 h at 60°C to remove Braun's lipoprotein. After heat-inactivation and washing, the samples were treated with muramidase (100 mg/ml) for 16 h at 37°C, in 50 mM phosphate buffer, pH 4.9. Muramidase digestion was boiled and centrifuged and the supernatants were reduced with 0.5 M sodium borate pH 9.5 and sodium borohydride. Finally, samples were adjusted to pH 3.5 with phosphoric acid.

Chromatographic separation was performed as previously described (van der Aart et al., 2018) on an Acquity UPLC HSS T3 C18 column (1.8 µm, 100 Å, 2.1 × 100 mm).

The peak areas of masses corresponding to muropeptides were collected and a final table which shows peak areas as percentage of the whole was produced in Microsoft Excel.

Proteomic Analysis

Equal amounts of *V. cholerae* O1 biovar El Tor str. N16961 cells from biological triplicate LB overnight cultures or VBNC microcosms were collected using centrifugation. Cells were carefully washed with ice-cold PBS and subjected to proteomic analysis using mass spectrometry (MS). In the first step, cell pellets were reconstituted in 2% Sodiumlauroylsarcosinate and heated for 15 min at 95°C. Protein concentration was measured and 50 µg of total solubilized protein was used for further analysis. The samples were incubated with 5 mM tris(2-carboxyethyl)phosphine at 95°C for 15 min followed by 30 min incubation with 10 mM iodoacetamide at 25°C. For in-solution digestion (ISD), the samples were diluted to 0.5% detergent using 100 mM NH4HCO3. One Micro gram trypsin (Promega) was used for digestion overnight at 30°C. Prior to Liquid Chromatography-Mass Spectrometry (LC-MS) analysis, samples were acidified and purified using C18 microspin columns (Harvard Apparatus) according to the manufacturer's instructions.

Using the protein digests of the biological triplicate samples, LC-MS/MS analysis was performed on Q-Exactive Plus mass spectrometer connected to an electrospray ion source (Thermo Fisher Scientific). Peptide separation was carried out using Ultimate 3000 nanoLC-system (Thermo Fisher Scientific), equipped with packed in-house C18 resin column (Magic C18 AQ 2.4 µm, Dr. Maisch). The peptides were first loaded onto a C18 precolumn (preconcentration set-up) and then eluted in backflush mode with a gradient from 98 % solvent A (0.15 % formic acid) and 2 % solvent B (99.85 % acetonitrile, 0.15 % formic acid) to 25 % solvent B over 105 min, continued from 25 to 35 % of solvent B up to 135 min. The flow rate was set to 300 nL/ min. The data acquisition mode for the initial label-free quantification study was set to obtain one high-resolution MS scan at a resolution of 60,000 (m/z 200) with scanning range from 375 to 1500 m/z followed by MS/MS scans of the 10 most intense ions. To increase the efficiency of MS/MS shots, the charged state screening modus was adjusted to exclude unassigned and singly charged ions. The dynamic exclusion duration was set to 30 s. The ion accumulation time was set to 50 ms (both MS and MS/MS). The automatic gain control (AGC) was set to 3×10^6 for MS survey scans and 1×10^5 for MS/MS scans.

For label-free quantification the MS raw data were analyzed with Progenesis QI software (Non-linear Dynamics, version 2.0). MS/MS search of aligned LC-MS runs was performed using MASCOT against a decoy database of the uniprot *Vibrio cholerae* protein database (UniProt Consortium, 2018). The following search parameters were used: full tryptic specificity required (cleavage after lysine or arginine residues); two missed cleavages allowed; carbamidomethylation (C) set as a fixed modification; and oxidation (M) set as a variable modification. The mass tolerance was set to 10 ppm for precursor ions and 0.02 Da for fragment ions for high energy-collision dissociation (HCD). Results from the database search were imported back

to Progenesis, mapping peptide identifications to MS1 features. The peak heights of all MS1 features annotated with the same peptide sequence were summed, and protein abundance was calculated per LC-MS run. Next, the data obtained from Progenesis were evaluated using SafeQuant R-package version 2.2.2 (Glatter et al., 2012). Hereby, 1% false discovery rates (FDR) of identification and quantification as well as intensity-based absolute quantification (iBAQ) values were calculated.

To further gain more information on the detected proteins, their localization was predicted using PSORTdb (Peabody et al., 2016) and Fur binding boxes were inferred from Panina et al. (2001); Mey et al. (2005). Data from a microarray study (Asakura et al., 2007) and RNA sequencing analysis (Xu et al., 2018) of *V. cholerae* VBNC cells are included for comparison (see **Table S3**). In addition, the abundance of predicted enzymes of metabolic pathways were mapped using the Kyoto Encyclopedia of Genes and Genomes (KEGG) database (Kanehisa and Goto, 2000; Kanehisa et al., 2017) (see **Table S5**). Finally, the proteomic data was further sorted according to their predicted regulons as inferred from RegPrecise 3.0 (Novichkov et al., 2013).

RESULTS

V. cholerae Enters the VBNC State After Prolonged Incubation

In order to simulate the aquatic habitats as closely as possible in our laboratory setting, we used water samples collected from environmental sources, including fresh water (NFW), brackish water (NBW) and salt water (NSW). Cells introduced into the 50 ml microcosms of NFW, NBW and NSW had all lost their ability to form colonies on LB plates over the course of 200 days (**Figure 1**). At the final time point 69% (NFW), 70% (NBW) and 65% (NSW) of the cells were viable according to live/ dead staining with Syto9 and propidium iodide (data not shown). From the initial $\sim 2 \times 10^9$ cells/ ml the final total cell count showed a reduction of the cells per ml to $6.3 \times 10^6 \pm 2.4 \times 10^6$ (NFW), $2.8 \times 10^7 \pm 1.2 \times 10^7$ (NBW) and $1.3 \times 10^7 \pm 3.3 \times 10^6$ (NSW) (**Figure 1**, dashed lines).

Biochemical Analysis of Osmoregulated Periplasmic Glucans and Peptidoglycan

The transfer of the LB ON cultures to the respective water samples causes an osmotic up- or downshift in our cell cultures. Therefore, we analyzed the presence and quantity of osmoregulated periplasmic glucans (OPGs), which are a known response to changes of environmental osmolarity in growing cells (Bohin, 2000). *V. cholerae* from LB ON cultures used to inoculate the natural water microcosms contained 0.37 μg OPGs/ mg cell weight, while cells grown in LB with no NaCl contained 1.13 μg OPGs/ mg, and cells from LB +30 g NaCl/ l contained 0.20 μg OPGs/ mg cells, respectively. The VBNC cells were all within the range of the value of the inoculum with 0.27 μg OPGs/ mg cells (NFW), 0.17 μg/ mg cells (NBW) and 0.25 μg/ mg cells (NSW) indicating either a lack of OPG production or immediate cession of growth.

The change from "comma"-shaped to small, round cells suggests that the peptidoglycan (PG) may be remodeled between these two states. To test this hypothesis, we analyzed digested murein sacculi by LC-MS (**Table S1** and **Figure S2**). Of monomeric muropeptides, the amount of tetrapeptides increased from 70.3% in stationary cells to 79.4% in VBNC cells. Similarly, the amount of TetraTetra dimers increased from 38.3% in stationary cells to 62.3% in VBNC cells. The PG of both cell types contains low amounts of D-methionine (10% in stationary cells and 6% in VBNC). The amount of muropeptides carrying an anhydro-group at the N-acetylmuramic acid (MurNAc) moiety was similar between the two cell types, indicating that the length of the glycan strands was generally similar. No pentapeptides were detected in the VBNC cells, which corresponds well to the observed lack of growth. Furthermore, comparison of the base peaks of disaccharides vs. bi-disaccharides of both sets, showed that cells from LB ON cultures cells carried 20% more cross-links than the VBNC cells.

General Morphological and Physiological Changes

Electron cryo-tomography of *V. cholerae* VBNC cells revealed their characteristic morphology; these small, round cells contain a cytoplasmic compartment of reduced volume and are devoid of storage granules, independent of the water used for incubation (**Figure 2A**, **Figure S1** and **Movies S1–S4**). Of the observed cells, 14% (NBW), 20% (NSW), and 22% (NFW) had a damaged cytoplasmic membrane (CM), resulting in loss of cytosolic content (for examples, see **Figure S1**). These cells were deemed "dead" and were excluded from the subsequent analysis.

In 29% of all VBNC cells, we observed up to five convex patches in the OM, containing two pronounced layers that differ from the typical OM of *V. cholerae* (**Figures 2A,B**). These were never observed in standard overnight LB (LB ON) lab culture cells. Using line scans perpendicular to the membranes, the thickness and spacing between the two layers was determined. We found that the OM patches closely resemble the appearance of the flagellar sheath membrane (**Figures 2C,D**).

A characteristic feature of the CM was the presence of multiple invaginations into the cytoplasm that were at least partially open to the periplasm (**Figures 2E,F**). These invaginations were found in VBNC cells from NBW and NSW microcosms as well as in cells raised in overnight LB cultures, but not in cells incubated in NFW.

Multiple large proteinaceous structures required for important cellular behaviors such as sensing, motility, attachment and secretion are embedded in the cellular envelope. Since an expansion of the periplasmic space is characteristic for VBNC cells, the functionality or synthesis of these envelope embedded complexes may be affected in the VBNC cells. Thus, we next focused on determining if they are still present and also if they retained their subcellular location (**Table 1**). ECT analysis revealed that many VBNC cells were flagellated. In 18% of all VBNC cells, the flagellar basal body or a pilus is contained in a small vesicle and, thus, separated from the bulk cytoplasmic compartment (**Figure 2H**). The type IV pili (T4P) that we

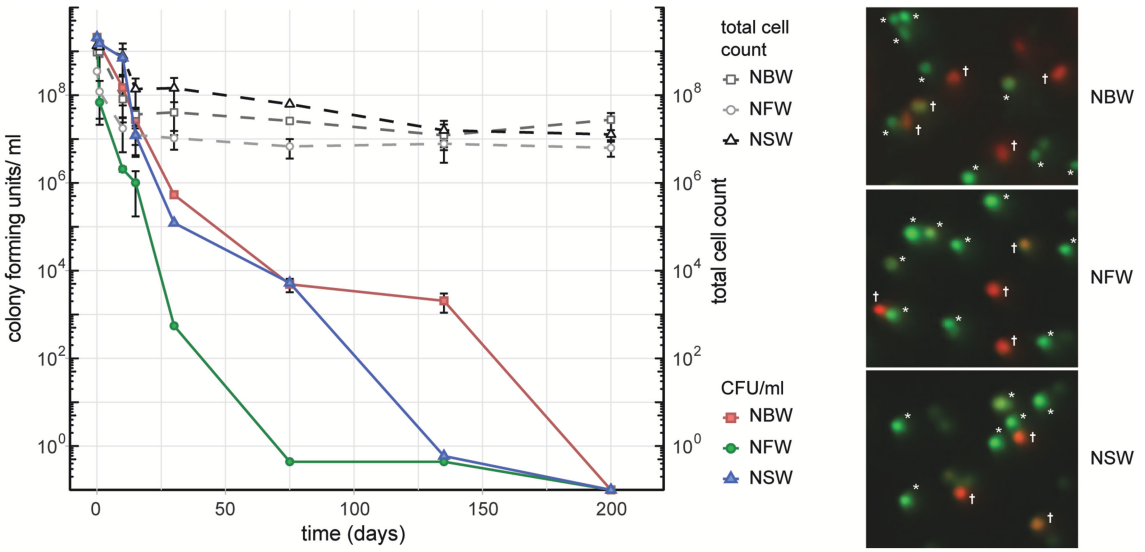

FIGURE 1 | Cell number, colony forming units (CFU) and viability during VBNC formation. **Left panel** shows the CFU/ ml and total cells count of *V. cholerae* incubated in natural brackish (NBW), fresh (NFW) or salt water (NSW). **Right panel** shows examples of the live/ dead staining using propidium iodide and Syto9. Cells marked with an asterisk were counted as "live" while cells with yellow, orange or red hue (marked with a cross) are deemed "dead".

observed in VBNC cells all had a diameter of ∼6 nm (**Figure 2I**) and are therefore unlikely to be TCP pili, which were previously determined to be ∼8 nm thick (Chang et al., 2017).

Of the three chemotaxis systems present in the *V. cholerae* genome (cluster I, II, and III), only cluster II chemosensory systems were found with similar abundance in cells of all incubation types. These can be clearly identified by the presence of periplasmic receptor domains, as well as the characteristic 25 nm spacing between the base plate and the inner membrane (Briegel et al., 2009). The cytoplasmic cluster I chemosensory system was only observed in a few cells incubated in NBW and NFW, while cluster III was not seen in any of the imaged cells.

Finally, we also observed a region characterized by a relatively homogeneous density and lack of ribosomes, which appears to be the considerably condensed chromosome (**Figure 2G**). Intriguingly, we only observed this in the cells from NSW and NBW incubations, but did not observe a similar DNA condensation in the VBNC cells from the NFW sample.

Proteomic Analysis of VBNC Cells

To gain more insights into changes associated with the VBNC state, the proteomes of VBNC cells and cells of an LB ON lab culture were compared.

Since many of the structural changes were highly similar in VBNC cells obtained from all types of water samples, NBW water cultures were used for proteomic analysis using mass spectrometry and label-free quantification. The respective names were inferred from Uniprot, and functional categories were assigned using KEGG and DAVID (Kanehisa and Goto, 2000; Huang da et al., 2009a,b; UniProt Consortium, 2018). Of the 2219 quantified proteins, 1349 were significantly over- or underrepresented ($q < 0.01$) in VBNC cells as compared to LB ON cells, demonstrating the extensive impact of the VBNC status on the cellular content (**Tables S2**, **S3**; **Figure S3**). Proteins that were detected with $n >= 3$ peptides were analyzed in more detail. Components that were more abundant in VBNC cells fell, among others, into the categories of bacterial chemotaxis, flagellar assembly, ribosomal proteins, arginine biosynthesis, and ABC transporters. Less abundant proteins in VBNC cells were predominantly allocated to metabolic categories such as carbon metabolism, tricarboxylic acid cycle (TCA) cycle, amino acid, amino sugar and nucleotide sugar metabolism (**Table S4**). For more detailed analysis, the components of individual structures or pathways were further refined using published data or the VchoCyc database (Shi et al., 2006).

Large Protein Complexes

In the proteomic analysis, we detected multiple proteins involved in the formation of T4P, flagellar and chemosensory systems with significant changes between LB ON cultures and VBNC cells (**Figure 3**).

The *V. cholerae* genome contains three T4P systems: the mannose-sensitive haemagglutinin (MSHA) pili, the toxin co-regulated pili (TCP) and the chitin co-regulated pili (ChiRP) (Taylor et al., 1987; Jonson et al., 1991; Fullner and Mekalanos, 1999; Aagesen and Häse, 2012). The MSHA and ChiRP systems are both T4a pili, while the TCP are T4b pili (Chang et al., 2017). The seven detected MSHA pili proteins presented only a slightly lower or higher abundance in VBNC compared to LB ON cells or were not significantly different between the cultures. Very few proteins of the other two pili systems were detected. Of those, TCP biosynthesis protein TcpF levels in VBNC cells was not significantly different from LB ON cultures, but all other TCP and ChiRP components were less abundant.

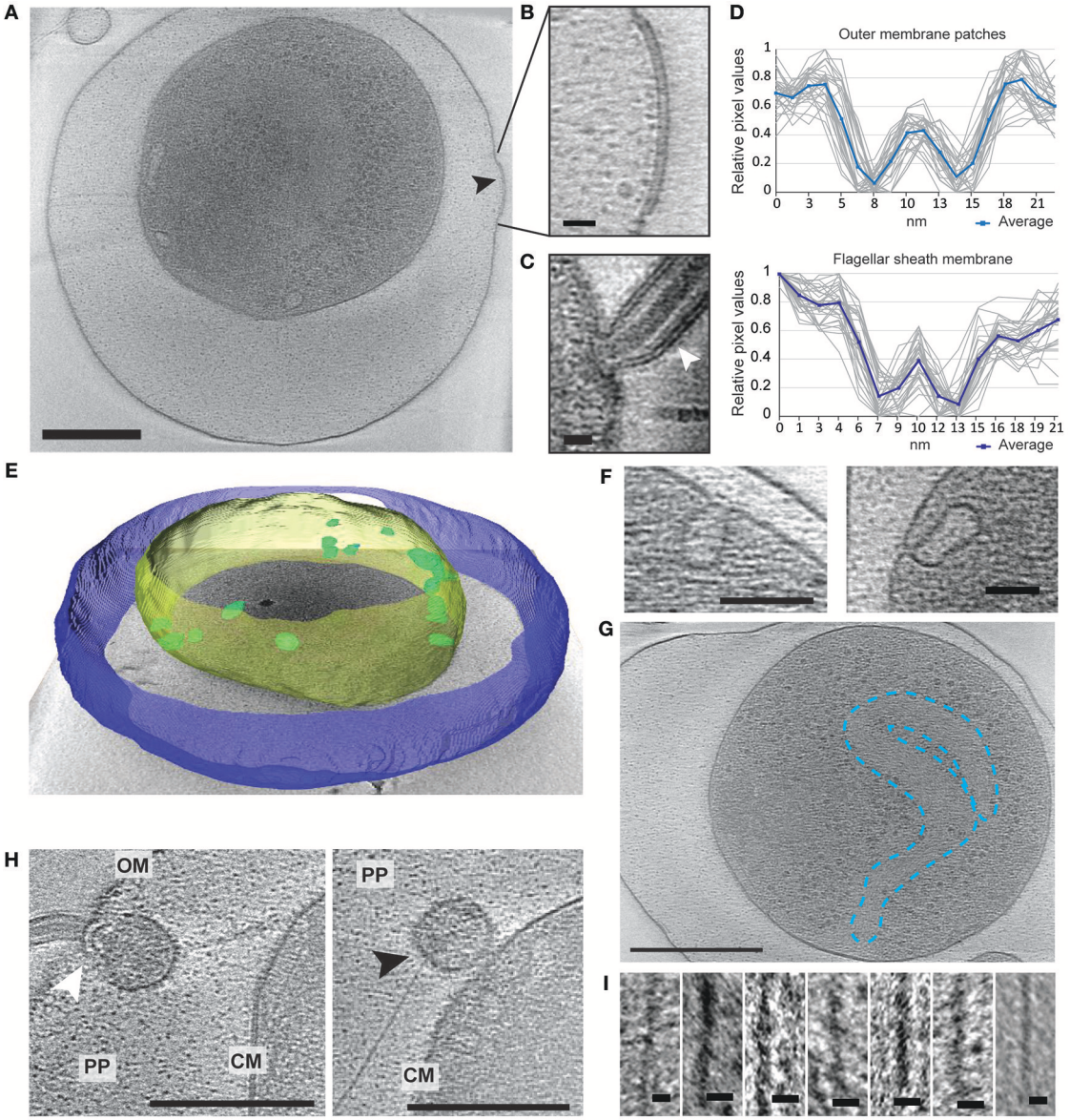

FIGURE 2 | Structural changes of VBNC cells as observed by ECT. **(A)** A cell from a NBW microcosm with a convex OM patch (black arrow). **(B)** Magnified detail of A exhibiting the pronounced two layers of the OM patch. **(C)** Flagellar sheath membrane (white arrow) for comparison. **(D)** Individual (gray) and averaged (blue) line scan measurements perpendicular to the membrane exhibit similar spacing of the two layers in the outer membrane patch (upper panel) and flagellar sheath membrane (lower panel). **(E)** Tomogram of a NBW VBNC cell segmented using Amira. Outer membrane (blue) is clearly separated from the cytoplasmic membrane (yellow). Multiple invaginations (green) can be found lining the cytoplasmic membrane. **(F)** Examples of the invaginations found in VBNC cells from NBW (left panel) and NSW (right panel) microcosms. **(G)** Tentative outline highlighting the condensed chromosomal DNA. **(H)** VBNC cells showing flagella (left panel, white arrow) or T4P (right panel, black arrow) embedded in small vesicles. **(I)** Details of exemplary T4P. Scale bars represent 200 nm **(A,G)**, 100 nm **(H)**, 50 nm **(F)** and 10 nm **(B,C,I)**, respectively. CM, cytoplasmic membrane; PP, periplasm; OM, outer membrane.

V. cholerae moves through the environment using flagellar rotation guided by chemotaxis. Seven out of 19 detected flagellar proteins showed a >1.5 - fold abundance, further 10 were represented at similar levels as in LB ON cells and only the flagellar biosynthesis proteins FlhF and FlhA were significantly less abundant in VBNC cells. Flagellar motility is controlled by the chemosensory cluster II. Five of the 40H class methyl-accepting chemosensory proteins (MCPs) associated with cluster II were >1.5 – fold more abundant while three were 1.5-fold reduced. The remaining 22 detected cluster II components, including the kinase CheA and chemotaxis protein CheW, showed only minor changes. As observed in the ECT data, a fraction of the VBNC cells from NBW microcosms contained cluster I chemosensory arrays which is in line with the increased

TABLE 1 | Quantification of occurrence of structures in cells from VBNC microcosms and LB ON cultures as observed by ECT.

Sample	N	Flagella	Chemosensory system			T4P	Detached OM	Condensed DNA
			I	II	III			
NBW	35	66%	9%	71%	-	23%	100%	83%
NFW	18	33%	6%	94%	-	72%	100%	-
NSW	18	39%	-	72%	-	22%	100%	83%
LB ON	18	72%	-	83%	-	33%	17%	-

abundance of the cluster I chemosensory array CheA (VC1397), CheW (VC1402), and the MCP DosM (VC1403) in these cells.

Pathogenicity

The flagellum as well as adhesins such as OmpU (VC0633), GbpA (VCA0811), FrhA (VC1620) and Mam7 (VC1501) are required for successful initial attachment to the intestinal epithelium (Attridge and Rowley, 1983; Sperandio et al., 1995; Kirn et al., 2005; Syed et al., 2009; Krachler et al., 2011). Only OmpU and Mam7 were detected in the proteomic analysis, exhibiting a similar (OmpU) or slightly higher abundance (Mam7) in the *V. cholerae* VBNC state than in LB ON cells.

Following the initial colonialization, a plethora of other virulence factors and regulators are known or likely to be involved in pathogenicity of *V. cholerae*. This includes the TCP pilus, the cholera toxin CtxAB, the type II secretion system (T2SS) proteins EpsCDEFGHIJKLMN, hemolysin A, ten further predicted hemolysins or hemolysin secretion proteins, the accessory colonization factor AcfBC, the MARTX toxin, Zot and Ace toxins (as reviewed for example in Childers and Klose, 2007; Almagro-Moreno et al., 2015; Conner et al., 2015; Silva and Benitez, 2016). Only 15 of these were detected with more than two peptides in the MS analysis. Of these, only the putative hemolysin secretion protein VC0199, a putative hemolysin (VC0578), the hemolysin Hlx VCA0594 and the T2SS proteins EpsCEFGL were found with a slightly increased abundance in VBNC cells (**Figure 4**).

Envelope Maintenance, Cell Shape and Division

Contrary to the drastic morphological changes of the envelope of VBNC cells, half of the proteins involved in cell division, cell shape and the synthesis and maintenance or structure of the cell envelope were not significantly more or less abundant (**Figure S4**). If we observed differences, these changes differed only slightly between the cultures (up to $\pm$1.5 fold). This includes the proteins that determine the rod-shape (MreBC) and curvature of the cell (CvrA). The two enzymes predicted to be responsible for OPG production, MdoHG (VC1287 and VC1288) were less abundant than in cells grown in LB ON cultures.

Metabolic Enzymes

VBNC cells have previously been reported to exhibit a markedly restrained metabolism (Mederma et al., 1992; Rahman et al., 1994; Oliver et al., 1995; Morishige et al., 2015). To analyze potential shifts in metabolic pathways, we retrieved the predicted function of metabolic proteins detected in the VBNC proteome data, mapped their respective pathways and expected underlying regulons using KEGG, VchoCyc and RegPrecise 3.0 (Kanehisa and Goto, 2000; Shi et al., 2006; Novichkov et al., 2013; Kanehisa et al., 2017) (**Tables S5**, **S6**). Cell envelope proteins involved in electron transport such as cytochromes (VC1442, VC1441, VC1440, VC1439, & VC1951), formate dehydrogenases (VC1519, VC1511, & VC1512) and cytochrome d ubiquinol oxidases (VC1843 & VCA0872) were less abundant in VBNC cells. We observed a significant reduction of enzymes involved in the central carbohydrate metabolism, specifically those required for glycolysis, the TCA cycle and the pentose phosphate pathway. Furthermore, we found a reduction of proteins predicted to be involved in the biosynthesis of lipopolysaccharides, isoprenoids, nucleotides and branched-chain amino acids as well as of co-factors such as riboflavin, NAD, ubiquinone and glutathione. In contrast, proteins of the Entner-Doudoroff (ED) pathway, the urea cycle and fatty acid β-oxidation were more abundant in VBNC cells. In addition, components of the amino acid metabolism, as well as the siderophore and iron-sulfur cluster biosynthesis, were increased. Predicted ABC transporters with at least two components significantly more abundant, were those involved in up-take of sulfate, iron (III), arginine/ornithine, L-amino acids and oligopeptides (**Table S7**).

Since the components of the mentioned pathways are often part of the same regulon(s), we next analyzed their abundance in relation to the regulatory networks. Genes that are upregulated in *V. cholerae* O395 by low iron availability and/ or the absence of master regulator Fur, or contained a predicted Fur binding box in their upstream region, were used to define the subclass of iron/Fur regulated proteins (**Figure 5**) (Panina et al., 2001; Mey et al., 2005). With the exception of a ferroxidase (VC0365) and a protein putatively involved in iron uptake (VC1264), all other proteins whose genes are repressed by Fur are present in higher concentrations in VBNC. This also includes the gene for manganese-dependent superoxide dismutase SodA, while the iron-dependent superoxide dismutase SodB was two-fold less abundant. Proteins encoded by genes that are either activated by Fur or not part of its regulon (VCA0678, VCA0679, VC1516, VCA0784, and VC1216) were found in lower or only slightly higher abundance in VBNC cells. Proteins encoded by genes with a predicted upstream Fur binding box in their upstream region, but without expression data from a Fur mutant, showed a mixed pattern.

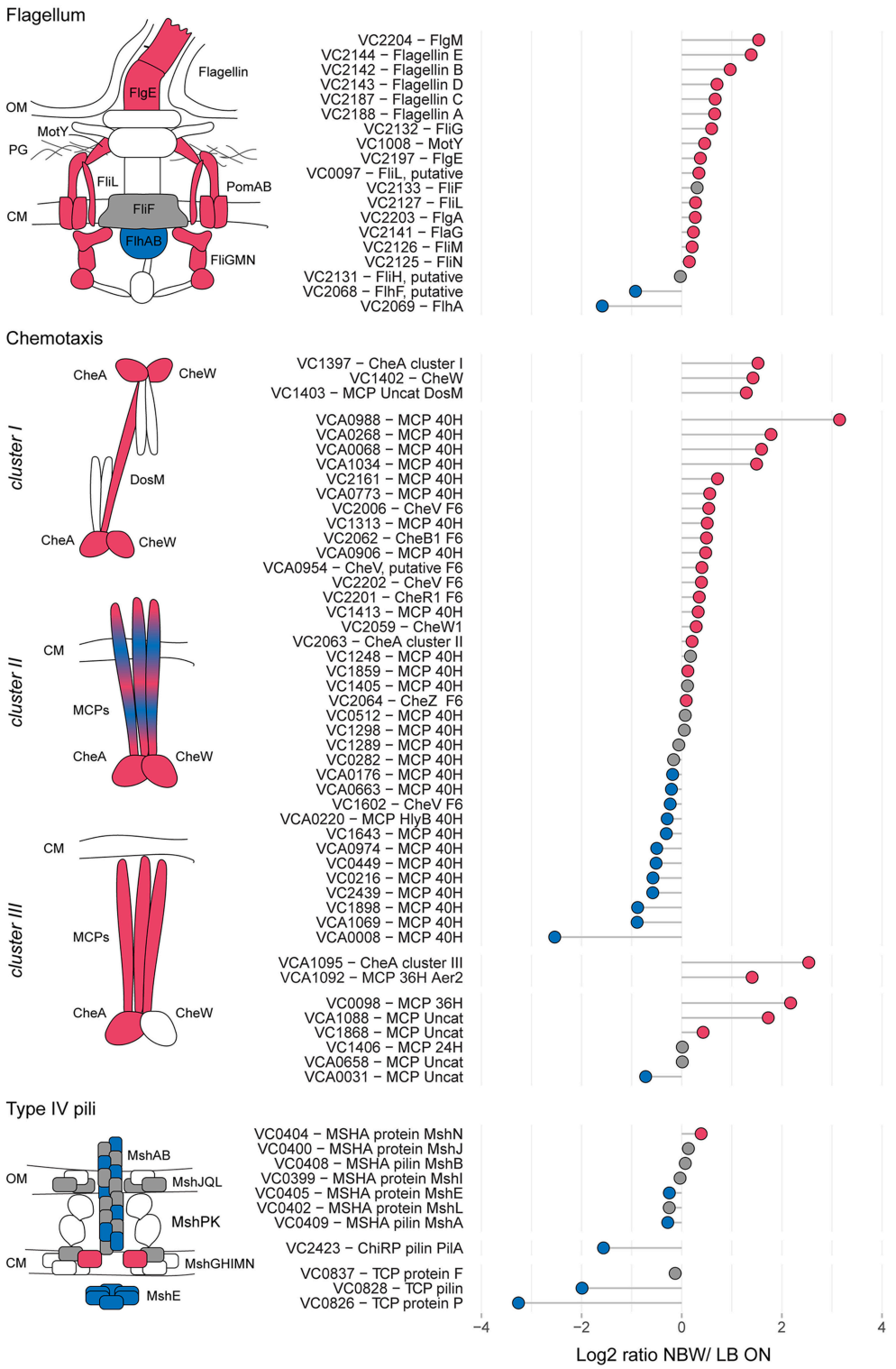

FIGURE 3 | Relative protein abundances of components of the flagellum, chemotaxis arrays and T4P. The left illustrations depict which components of the respective structures are more (red) or less (blue) abundant or not significantly different (gray). White symbols represent components that were not found in the MS analysis or with peptides $n < 2$. CM, cytoplasmic membrane; OM, outer membrane. Depicted is the $\log_2$-ratio of NBW VBNC cells and LB ON cells. Proteins found in significantly higher abundance in VBNC cells compared to LB ON are indicated by red circles while significantly lower ratios are shown as blue circles. Gray circles represent components with no significant difference between VBNC and LB ON cells ($q < 0.01$). Chemotaxis components are grouped by their predicted interaction with the respective chemosensory cluster.

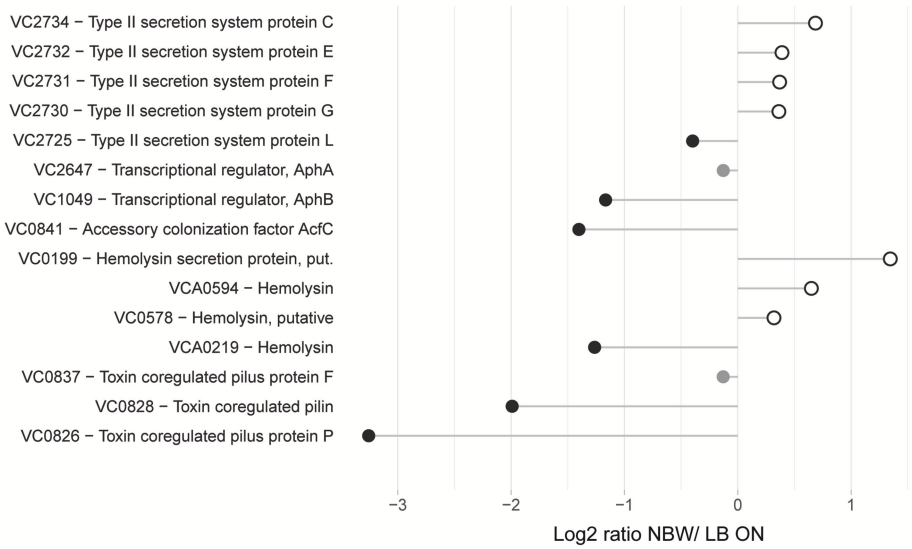

FIGURE 4 | Relative protein abundances of proteins associated with pathogenicity. Depicted is the $\log_2$-ratio of NBW VBNC cells and LB ON cells. Proteins found in significantly higher abundance in VBNC cells compared to LB ON are indicated by open white circles while significantly lower ratios are shown as black circles. Protein abundances that were not significantly different are colored gray ($q < 0.01$).

Besides the already described Fur regulon, all proteins whose genes are predicted to be repressed by ArgR, GntR, IscR, and TyrR, as well as those for the repressors themselves, were more abundant. Genes that are predicted to be repressed by FruR, GalR, NanR, PdhR, PrpR, and ScrR showed a decrease in expression, as based on the proteome data. With the exception of NanR, all these repressors were also less abundant. The remaining regulons showed a mixed pattern with varying protein levels of their regulons.

DISCUSSION

In between seasonal outbreaks of cholera, *V. cholerae* resides in environmental water bodies. In environmental samples, plate counts frequently resulted in lower cell numbers of the pandemic *V. cholerae* O1 serotype than direct enumeration methods. This indicates that at least parts of the *V. cholerae* population is in the viable but non-culturable state in the tested waters (Colwell et al., 1985; Huq et al., 1990; Hasan et al., 2002). After ingestion of *V. cholerae* VBNC cultures by human volunteers, the cells revert to the cultivable and infectious state, making them a potential threat to the public health (Colwell et al., 1996). Besides influencing the physiology and behavior of individual *V. cholerae* cells, environmental niches may have been important drivers in the evolution of the pandemic strains as they allowed recombination events with other pathogenic or non-pathogenic donors. Detailed studies of strains of the 7th cholera pandemic, of which the N16961 strain is a representative, and its pre-pandemic relatives demonstrated the step-wise acquisition of pathogenic traits through mutations, phage predation and recombination events during the first half of the 20th century (Mutreja et al., 2011; Hu et al., 2016). The notable decrease of recombination events in the 7th pandemic strains after 1961 could at least partially be attributed to the inactive VBNC life style of *V. cholerae* under suboptimal conditions (Hu et al., 2016). Thus, the VBNC phenotype not only enables the survival of pandemic strains in the environment and present a threat to the public health, but may also slow down its subsequent diversification. Understanding the VBNC phenotype in *V. cholerae* is therefore important to understand seasonal outbreaks as well as the further development of this species.

In this present study, cells that have reached the VBNC state have been subject to osmolarity up- or downshifts, low temperature and starvation for extended periods of time. The transition from warm LB cultures to natural waters resembles the osmolarity shifts experienced by *V. cholerae* when being shed by a human patient into the environment as the conductivity of LB broth and rice-stool water is similar (Nelson et al., 2008). As a result of these cultivation changes, the cells have undergone a process of drastic physiological and morphological restructuring.

Several features such as the overall loss of the vibrioid shape, a similarly small cytoplasm that was devoid of storage granules and the separation of the CM and OM occurred in all three water types (see **Figure S5**). The reduced cell size could potentially be created during cytoplasm shrinkage. Here, the flagellum, pili and other membrane spanning structures could act as tethers that anchor the CM to the OM. This, in turn, could lead to the observed second cytoplasmic compartments of smaller size. Despite these similar features, the cells incubated in fresh water showed noticeable differences to the cultures with higher salt concentrations. For example, *V. cholerae* in fresh water microcosms exhibited the lowest number of flagellated cells and a comparably high percentage of piliated cells, indicating that the water composition promotes different survival strategies.

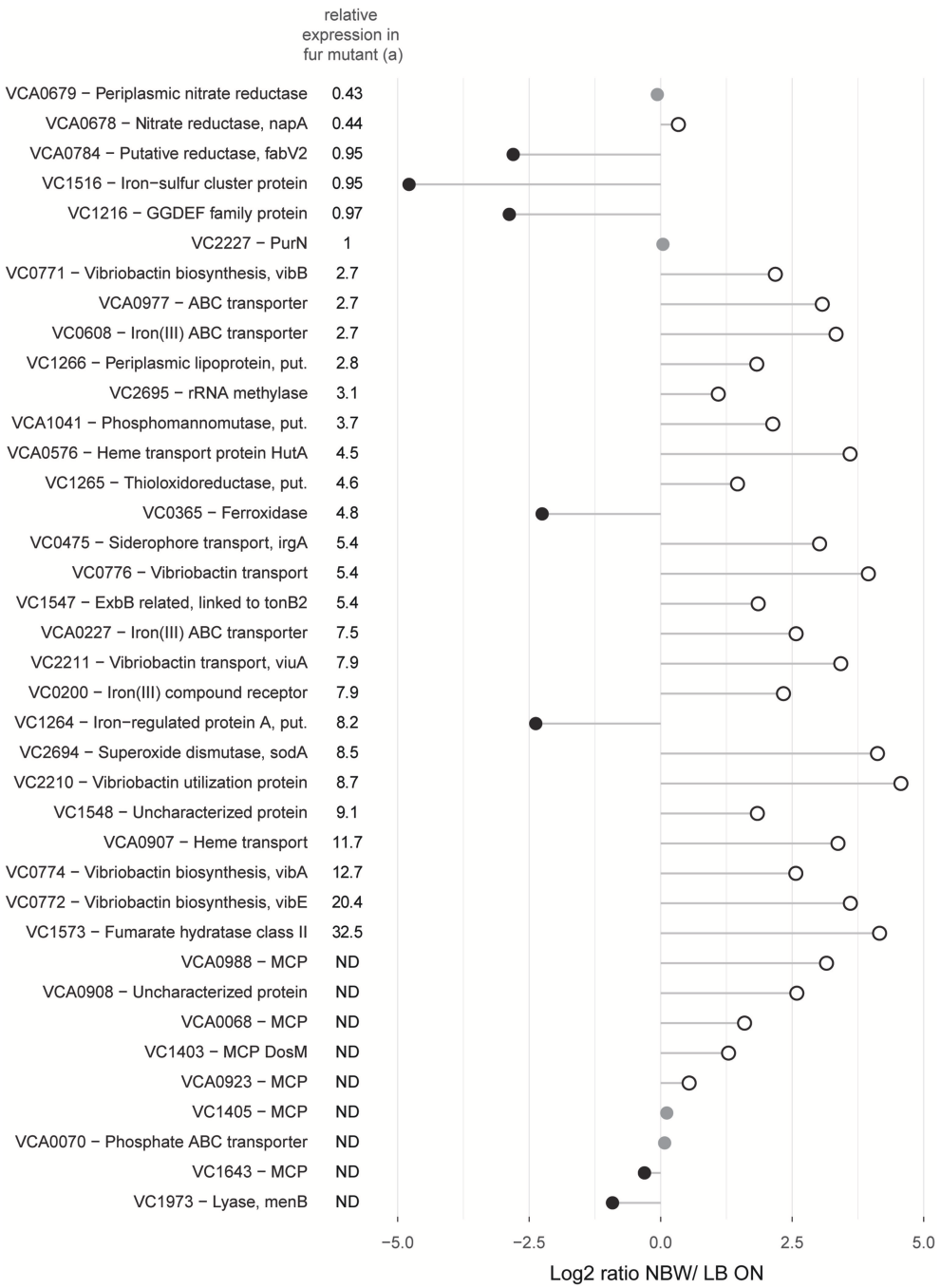

FIGURE 5 | Relative abundances of proteins with predicted Fur binding boxes in their upstream region and/ or shown regulation by iron availability and/ or the master regulator Fur. Depicted is the $\log_2$-ratio of NBW VBNC cells and LB ON cells. Proteins found in significantly higher abundance in VBNC cells compared to LB ON are indicated by open white circles while significantly lower ratios are shown as black circles. Protein abundances that were not significantly different are colored gray ($q < 0.01$). (a) Relative expression data was taken from Mey et al. (Mey et al., 2005). The genes of the first five proteins were positively regulated by iron and independently of Fur while the following 24 components were negatively regulated by Fur and iron. ND, not defined.

V. cholerae is frequently isolated from estuarine and salt water environments, but can also grow in fresh water if it contains sufficient assimilable organic carbon (Miller et al., 1982; Singleton et al., 1982a,b; Vital et al., 2007). Incubated in nutrient-poor lake water at room temperature for extended periods of time promotes the switch to a "persister" phenotype and biofilm formation (Jubair et al., 2012, 2014). Although the flagellum, the MSHA pilus and adhesins synergistically promote initial

surface attachment, the general switch from a flagella-driven, motile life style to a sessile, biofilm-forming one is inversely regulated through the messenger molecule cyclic diguanylate (Jenal and Malone, 2006; Liu et al., 2010; Utada et al., 2014). Thus, a decrease of flagella and increase of T4P could indicate that the cells incubated in NFW attempted to switch from the planktonic to a biofilm lifestyle during the transition to the VBNC state.

In general, the abnormal distance between CM and OM may disrupt a variety of processes such as envelope maintenance, sensing and motility as previously shown for *E. coli* (Asmar et al., 2017). The lack of structural conservation of the OM, CM and PG is likely due to the increased gap of the periplasm, rather than the absence of the maintenance machinery, as the detected proteins required for envelope maintenance and shape exhibited either unchanged or only minor differences in VBNC cells. One possible result could be the thick, convex patches of the OM that are reminiscent of the flagellar sheath. In Gram-negative bacteria, the asymmetric composition of the OM is tightly regulated to maintain its barrier function (see review by May and Silhavy, 2017). Aberrations, such as the convex OM patches, might be symptomatic of a perturbed OM maintenance in the VBNC state. Contrary to the radical change of the general morphology of *V. cholerae* VBNC, the PG alterations are rather subtle. No pentapeptides, indicative of lack of cell wall synthesis, were detected. The PG appeared less cross-linked in VBNC cells, while the glycan strands had a similar length as in PG obtained from LB ON cells. This is in contrast to the substantially higher rate of cross-linking, as well as shorter glycan strands, that were reported for *E. coli* VBNC cells (Signoretto et al., 2002). The authors speculated that especially the shorter glycan strands contribute to the formation of coccoid cells. In *V. cholerae* VBNC cells, the rounded cell shape may arise due to the lower degree of cross-linking of the PG which reduces cell wall stiffness (Huang et al., 2008; Furchtgott et al., 2011).

The invaginations of the CM found in cells incubated in NBW, NSW and LB ON incubations may be the result of an increase in protein content relative to the lipid membrane. A similar mechanism has previously been reported in cells that overproduce membrane proteins (Lefman et al., 2004; Zhang et al., 2007; Arechaga, 2013). The low level of OPGs in the periplasm of NFW VBNC cells may weaken their osmoprotection and prevent the formation of invaginations as the CM might be more strained through increased turgor pressure. The described cell envelope anomalies may affect the synthesis and function of the envelope-spanning structures such as pili and the flagellum. Certain integral structures, such as the alignment subcomplex of T4P and the stators of the flagellum, span the distance from the CM to the PG and their proper placement is essential to the respective functions (Chun and Parkinson, 1988; De Mot and Vanderleyden, 1994; Ayers et al., 2009; Tammam et al., 2013; Leighton et al., 2015). Thus, the pili and flagella that reside either in the small cytoplasmic vesicles or at sites of an enlarged periplasmic gap are likely not functional because of the increased distance between the envelope layers. The pili found in the VBNC cells are likely MSHA pili. We base this conclusion on their measured width of about 6 nm which matches the previously reported diameter of T4a pili (Chang et al., 2017), as well as the stable presence of several MSHA pili components and decreased abundance of ChiRP and TCP system components in the proteomics analysis. A previous study showed that *V. cholerae* VBNC cells cultivated in artificial sea water at 5°C can attach to chitin particles and intestinal epithelial cells (Pruzzo et al., 2003). The observed presence of the flagellum, T4P and at least two adhesins may be sufficient to mediate such initial attachment.

In addition to the changes in the *V. cholerae* VBNC cell envelope, we found several changes in the protein content of the cytoplasm. *V. cholerae* encodes three distinct chemotaxis systems (cluster I, II, III) and 44–45 different MCPs (Briegel et al., 2014). The MCPs that are known to interact with cluster II all belong to the 40H class (Briegel et al., 2009, 2016). Cluster II arrays sense a plethora of cues and are so far the only chemosensory system that control the chemotactic swimming behavior of *V. cholerae* (Gosink et al., 2002). This array is present in both VBNC and LB ON cells at similar frequency and with comparable CheA levels, but it seems to undergo restructuring based on the differences of the 40H MCP abundance. A recent study of *V. cholerae* cluster II revealed that this array is not ultrastable like in the case of *E. coli* chemotaxis arrays (Yang et al., 2018). This may facilitate MCP turn over and allow this species to quickly remodel this system to tune their chemotactic response. As the molecules sensed by individual MCPs are still unknown for most MCPs, the cues that these restructured cluster II arrays can sense remain to be uncovered. Cluster I chemosensory arrays were only observed in VBNC cells where the respective proteins were also 2.4–2.8 times more abundant. These arrays have been reported to be formed under low-oxygen conditions (Hiremath et al., 2015). As our cells were incubated in closed microcosms, they likely experienced oxygen depletion, which we assume induced the cluster I formation. Furthermore, we also observed a homogenous region in the cytoplasm that is reminiscent of the compact nucleoid of other bacteria (Pilhofer et al., 2010; Butan et al., 2011). Thus, we believe this region to be the condensed chromosomal DNA. Multiple proteins are capable of structuring and condensing DNA. Out of these, the IHF subunits and DPS were significantly more abundant in VBNC cells. Together, these proteins could be responsible for observed compacting the chromosome. However, DNA condensation is thought to be an interplay between molecular crowding and DNA structuring proteins (de Vries, 2010). This might explain why the compacted DNA was not observed in fresh water treated cells.

Similar to the absence of TCP pili, most other known pathogenicity factors were either not detected or showed similar or lower abundance in the proteomic analysis of VBNC cells. This included adhesins for initial attachment as well as the cholerae toxin and hemolysin A. Previous studies with *V. cholerae* strains concluded that VBNC cells retain their pathogenic potential based on the up-regulation of pathogenicity factor transcripts (Vora et al., 2005; Asakura et al., 2007; Mishra et al., 2012; Xu et al., 2018) or the presence of TCP pili (Krebs and Taylor, 2011). However, these studies are difficult to compare as each used different combination of strains (*V. cholerae* O395 or *V. cholerae* O1 strains N16961, El2382 or P6973), pre-cultures were either stationary or exponentially growing cultures from

different media (LB, TSB, or peptone water), VBNC inducing conditions (spent media at 30°C, lake water at 4°C, aerated or standing artificial sea water with 1%. 2.5 or 4% salt concentration at 4°C), incubation times (9–157 days) and starting CFUs (10^6/ ml−10^9/ ml). All of these factors may influence the expression pattern and pathogenic potential of the VBNC cultures. In addition, the observed increased transcripts may not result in elevated levels of the respective proteins due to inhibition of translation by ribosomal binding factors such as Vrp or HPF (Wada et al., 2006; De Bari and Berry, 2013; Sabharwal et al., 2015). To date, a single trial with nine participants determining the infectivity of *V. cholerae* VBNC cells has been published. Only one of the volunteers developed cholera symptoms. However, the authors noted that the loss of pathogenicity may be dependent on how long the cells are already in the VBNC state (Colwell et al., 1996). A time course dependent determination of the presence of pathogenicity factors is, to date, still lacking.

V. cholerae VBNC cells not only restructure their morphology but also their metabolism. Our proteomic data shows that proteins of several entire predicted regulons or pathways exhibit abundance shifts. This indicates the restructuring of the metabolism caused by loss of repression of several regulons. This includes most elevated gene products predicted or shown to be repressed by Fur, ArgR, GntR, IscR, and TyrR (Panina et al., 2001; Mey et al., 2005; Novichkov et al., 2013). The carbon metabolism also seemed to undergo a broad shift as proteins involved in glucose utilization (PtsGHI) and the Embden–Meyerhof–Parnas-pathway (Pgi, TipA, GapA) were all less abundant, while the glyoxylate shunt components showed stable (AceA) or slightly higher levels (AceB). In addition, VC0285, a predicted key protein of the ED pathway, and several enzymes of FA degradation were detected with increased levels. Furthermore, several ABC transport systems implicated to take up amino acids or peptides were found at higher levels. This indicates a vast metabolic shift toward alternative energy sources. This seems logical as *V. cholerae* was shown to lose 88.7% of their carbohydrates within a few days of starvation (Baker et al., 1983).

A general question regarding VBNC formation is whether the observed changes are due to active regulation or passive mechanisms such as stalled synthesis or maintenance and stochastic decay. Our data suggests that many of the alterations observed in the *V. cholerae* VBNC cell envelope are not due to active restructuring, but rather to passive changes that may be due to the dehiscence of the two membranes caused by a shrinking cytoplasm. The metabolic changes, induction of the cluster I chemosensory system and restructuring of the cluster II array appear actively regulated and in dependence to effector and oxygen availability. Whether the lower abundance of toxins and the absence of the TCP pilus is an active downregulation cannot be assessed, but indicates that the infectious potential of *V. cholerae* VBNC cells is likely diminished.

A previous report by Kim et al. on *E. coli* VBNC populations concluded that VBNC cultures are mainly composed of dead cells, as the majority of cells appeared to have an empty cytosol (Kim et al., 2018). This observation solely relied on the analysis of chemically fixed, dehydrated, heavy metal stained, resin-embedded and thin sectioned cell material without the three dimensional context of the whole cells. Each of these sample preparation steps can introduce artifacts and destroy the delicate ultrastructure of bacteria (Diaz-Visurraga et al., 2010; Pilhofer et al., 2010). Our analysis of 3D tomograms of flash-frozen VBNC cells cannot confirm the statement by Kim et al. for *V. cholerae* VBNC cells, since we only observed cells with a damaged CM and cytosol leakage in 14–22% of the cases. This number resembles the dead fraction determined by the live/dead staining experiment.

Most previous work consists of individual aspects of VBNC formation and decoupled structural and proteomic or transcriptomic studies. Here, we have coupled the proteomic and structural analysis to give important new insights into the extensive changes this pathogen undergoes upon VBNC-inducing conditions. To further study the temporal progress of VBNC development, future studies should include the proteomic analysis along the entire time course of their formation.

AUTHOR CONTRIBUTIONS

SB and AB designed the research project. SB, LA, J-ML and TG collected data. All authors were involved in data analysis and drafting of the manuscript.

FUNDING

This work is part of the research programme Building Blocks of Life with project number 737.016.004, which is (partly) financed by the Netherlands Organisation for Scientific Research (NWO). SB was supported by a postdoctoral fellowship from the German Academy of Sciences Leopoldina.

ACKNOWLEDGMENTS

The authors acknowledge the support and the use of resources of Instruct-ERIC. Data acquisition was performed at the Netherlands Centre for Electron Nanoscopy in Leiden (NeCEN) with assistance from Dr. Christoph Diebolder. This study has been posted as a bioRxvid preprint (Brenzinger et al., 2018).

SUPPLEMENTARY MATERIAL

The Supplementary Material for this article can be found online at: https://www.frontiersin.org/articles/10.3389/fmicb.2019.00793/full#supplementary-material

Movie S1 | Vibrio cholerae cell raised in LB ON culture.

Movie S2 | VBNC cell from NFW microcosm.

Movie S3 | VBNC cell from NSW microcosm.

Movie S4 | VBNC cell from NBW microcosm.

REFERENCES

Aagesen, A. M., and Häse, C. C. (2012). Sequence analyses of type IV pili from vibrio cholerae, vibrio parahaemolyticus, and vibrio vulnificus. *Microb. Ecol.* 64, 509–524. doi: 10.1007/s00248-012-0021-2

Almagro-Moreno, S., Pruss, K., and Taylor, R. K. (2015). Intestinal colonization dynamics of *Vibrio cholerae*. *PLoS Pathog.* 11:e1004787. doi: 10.1371/journal.ppat.1004787

Alvarez-Ordóñez, A., Broussolle, V., Colin, P., Nguyen-The, C., and Prieto, M. (2015). The adaptive response of bacterial food-borne pathogens in the environment, host and food: implications for food safety. *Int. J. Food Microbiol.* 213, 99–109. doi: 10.1016/j.ijfoodmicro.2015.06.004

Arechaga, I. (2013). Membrane invaginations in bacteria and mitochondria: common features and evolutionary scenarios. *J. Mol. Microbiol. Biotechnol.* 23, 13–23. doi: 10.1159/000346515

Asakura, H., Ishiwa, A., Arakawa, E., Makino, S. I., Okada, Y., Yamamoto, S., et al. (2007). Gene expression profile of *Vibrio cholerae* in the cold stress-induced viable but non-culturable state. *Environ. Microbiol.* 9, 869–879. doi: 10.1111/j.1462-2920.2006.01206.x

Asmar, A. T., Ferreira, J. L., Cohen, E. J., Cho, S. H., Beeby, M., Hughes, K. T., et al. (2017). Communication across the bacterial cell envelope depends on the size of the periplasm. *PLoS Biol.* 15:e2004303. doi: 10.1371/journal.pbio.2004303

Attridge, S. R., and Rowley, D. (1983). The role of the flagellum in the adherence of Vibrio cholerae. *J. Infect. Dis.* 147:864–72. doi: 10.1093/infdis/147.5.864

Ayache, J., Beaunier, L., Boumendil, J., Ehret, G., and Laub, D. (2012). "Artifacts in transmission electron microscopy," in *Sample Preparation Handbook for Transmission Electron Microscopy* (New York, NY: Springer), 125–170.

Ayers, M., Sampaleanu, L. M., Tammam, S., Koo, J., Harvey, H., Howell, P. L., et al. (2009). PilM/N/O/P proteins form an inner membrane complex that affects the stability of the *Pseudomonas aeruginosa* type IV pilus secretin. *J. Mol. Biol.* 394, 128–142. doi: 10.1016/j.jmb.2009.09.034

Baker, R. M., Singleton, F. L., and Hood, M. A. (1983). Effects of nutrient deprivation on Vibrio cholerae. *Appl. Environ. Microbiol.* 46, 930–940.

Balakrish Nair, G., Bhadra, R. K., Ramamurthy, T., Ramesh, A., and Pal, S. C. (1991). *Vibrio cholerae* and other vibrios associated with paddy field cultured prawns. *Food Microbiol.* 8, 203–208. doi: 10.1016/0740-0020(91)90051-3

Bergkessel, M., Basta, D. W., and Newman, D. K. (2016). The physiology of growth arrest: uniting molecular and environmental microbiology. *Nat. Rev. Microbiol.* 14, 549–562. doi: 10.1038/nrmicro.2016.107

Blake, P. A., Rosenberg, M. L., Costa, J. B., Ferreira, P. S., Guimaraes, C. L., and Gangarosa, E. J. (1977). Cholera in Portugal, 1974: I. modes of transmission. *Am. J. Epidemiol.* 105, 337–43. doi: 10.1093/oxfordjournals.aje.a112391

Bohin, J. P. (2000). Osmoregulated periplasmic glucans in Proteobacteria. *FEMS Microbiol. Lett.* 186, 11–19. doi: 10.1016/S0378-1097(00)00110-5

Brenzinger, S., van der Aart, L. T., van Wezel, G. P., Lacroix, J.-M., Glatter, T., and Briegel, A. (2018). Structural and proteomic changes in viable but non-culturable Vibrio cholerae. *bioRxiv*. doi: 10.1101/433326

Briegel, A., Ladinsky, M. S., Oikonomou, C., Jones, C. W., Harris, M. J., Fowler, D. J., et al. (2014). Structure of bacterial cytoplasmic chemoreceptor arrays and implications for chemotactic signaling. *Elife* 2014, 1–16. doi: 10.7554/eLife.02151

Briegel, A., Ortega, D. R., Mann, P., Kjær, A., Ringgaard, S., and Jensen, G. J. (2016). Chemotaxis cluster 1 proteins form cytoplasmic arrays in *Vibrio cholerae* and are stabilized by a double signaling domain receptor DosM. *Proc. Natl. Acad. Sci. U S A.* 113, 10412–10417. doi: 10.1073/pnas.1604693113

Briegel, A., Ortega, D. R., Tocheva, E. I., Wuichet, K., Li, Z., Chen, S., et al. (2009). Universal architecture of bacterial chemoreceptor arrays. *Proc. Natl. Acad. Sci. U. S. A.* 106, 17181–17186. doi: 10.1073/pnas.0905181106

Butan, C., Hartnell, L. M., Fenton, A. K., Bliss, D., Sockett, R. E., Subramaniam, S., et al. (2011). Spiral architecture of the nucleoid in Bdellovibrio bacteriovorus. *J. Bacteriol.* 193, 1341–1350. doi: 10.1128/JB.01061-10

Cava, F., de Pedro, M. A., Lam, H., Davis, B. M., and Waldor, M. K. (2011). Distinct pathways for modification of the bacterial cell wall by non-canonical D-amino acids. *EMBO J.* 30, 3442–3453. doi: 10.1038/emboj.2011.246

Chaiyanan, S., Chaiyanan, S., Grim, C., Maugel, T., Huq, A., and Colwell, R. R. (2007). Ultrastructure of coccoid viable but non-culturable Vibrio cholerae. *Environ. Microbiol.* 9, 393–402. doi: 10.1111/j.1462-2920.2006.01150.x

Chang, Y. W., Kjær, A., Ortega, D. R., Kovacikova, G., Sutherland, J. A., Rettberg, L. A., et al. (2017). Architecture of the *Vibrio cholerae* toxin-coregulated pilus machine revealed by electron cryotomography. *Nat. Microbiol.* 2:16269. doi: 10.1038/nmicrobiol.2016.269

Childers, B. M., and Klose, K. E. (2007). Regulation of virulence in Vibrio cholerae: The ToxR regulon. *Future Microbiol.* 2:335–44. doi: 10.2217/17460913.2.3.335

Chun, S. Y., and Parkinson, J. S. (1988). Bacterial motility: membrane topology of the Escherichia coli MotB protein. *Science* 239, 276–278. doi: 10.1126/science.2447650

Colwell, R. R., Brayton, P., Herrington, D., Tall, B., Huq, A., and Levine, M. M. (1996). Viable but non-culturable *Vibrio cholerae* O1 revert to a cultivable state in the human intestine. *World J. Microbiol. Biotechnol.* 12, 28–31. doi: 10.1007/BF00327795

Colwell, R. R., Brayton, P. R., Grimes, D. J., Roszak, D. B., Huq, S. A., and Palmer, L. M. (1985). Viable but non-culturable *vibrio cholerae* and related pathogens in the environment: Implications for release of genetically engineered microorganisms. *Bio/Technology*. 3, 817–820 doi: 10.1038/nbt0985-817

Conner, J. G., Teschler, J. K., Jones, C. J., and Yildiz, F. H. (2015). Staying Alive: *Vibrio cholerae's* Cycle of environmental survival, transmission, and dissemination. *Microbiol. Spectr.* 4, 593–633. doi: 10.1128/microbiolspec.VMBF-0015-2015

De Bari, H., and Berry, E. A. (2013). Structure of *Vibrio cholerae* ribosome hibernation promoting factor. *Acta Crystallogr. Sect. F Struct. Biol. Cryst. Commun.* 69:228–236. doi: 10.1107/S1744309113000961

De Mot, R., and Vanderleyden, J. (1994). The C-terminal sequence conservation between OmpA-related outer membrane proteins and MotB suggests a common function in both Gram-positive and Gram-negative bacteria, possibly in the interaction of these domains with peptidoglycan. *Mol. Microbiol.* 12, 333–334. doi: 10.1111/j.1365-2958.1994.tb01021.x

de Vries, R. (2010). DNA condensation in bacteria: Interplay between macromolecular crowding and nucleoid proteins. *Biochimie.* 92:1715-1721. doi: 10.1016/j.biochi.2010.06.024

Diaz-Visurraga, J., Cardenas, G., and Garcia, A. (2010). Morphological changes induced in bacteria as evaluated by electron microscopy. *Microsc. Sci. Technol. Appl. Educ.* 307–315.

Fullner, K. J., and Mekalanos, J. J. (1999). Genetic characterization of a new type IV-A pilus gene cluster found in both classical and El Tor biotypes of *Vibrio cholerae*. *Infect. Immun.* 67:1393–404

Furchtgott, L., Wingreen, N. S., and Huang, K. C. (2011). Mechanisms for maintaining cell shape in rod-shaped gram-negative bacteria. *Mol. Microbiol.* 81, 340–353. doi: 10.1111/j.1365-2958.2011.07616.x

Glatter, T., Ludwig, C., Ahrn,é, E., Aebersold, R., Heck, A. J., and Schmidt, A. (2012). Large-scale quantitative assessment of different in-solution protein digestion protocols reveals superior cleavage efficiency of tandem Lys-C/trypsin proteolysis over trypsin digestion. *J. Proteome Res.* 11:5145–56. doi: 10.1021/pr300273g

González-Escalona, N., Fey, A., Höfle, M. G., Espejo, R. T., and Guzmán, C. A. (2006). Quantitative reverse transcription polymerase chain reaction analysis of *Vibrio cholerae* cells entering the viable but non-culturable state and starvation in response to cold shock. *Environ. Microbiol.* 8, 658–666. doi: 10.1111/j.1462-2920.2005.00943.x

Gosink, K. K., Kobayashi, R., Kawagishi, I., and Häse, C. C. (2002). Analyses of the roles of the three cheA homologs in chemotaxis of Vibrio cholerae. *J. Bacteriol.* 184, 1767–1771. doi: 10.1128/JB.184.6.1767-1771.2002

Guan, N., Li, J., Shin, H., Du, G., Chen, J., and Liu, L. (2017). Microbial response to environmental stresses: from fundamental mechanisms to practical applications. *Appl. Microbiol. Biotechnol.* 101, 3991–4008. doi: 10.1007/s00253-017-8264-y

Hasan, J. A. K., Montilla, R., Colwell, R. R., Chowdhury, M. A. R., Huq, A., and Xu, B. (2002). A simplified immunofluorescence technique for detection of viable cells of *Vibrio cholerae* O1 and O139. *J. Microbiol. Methods*. 24:165–70. doi: 10.1016/0167-7012(95)00066-6

Hiremath, G., Hyakutake, A., Yamamoto, K., Ebisawa, T., Nakamura, T., Nishiyama, S., et al. (2015). Hypoxia-induced localization of chemotaxis-related signaling proteins in *Vibrio cholerae*. *Mol. Microbiol.* 95, 780–790. doi: 10.1111/mmi.12887

Hu, D., Liu, B., Feng, L., Ding, P., Guo, X., Wang, M., et al. (2016). Origins of the current seventh cholera pandemic. *Proc. Natl. Acad. Sci. U.S.A.* 113:E7730-E7739. doi: 10.1073/pnas.1608732113

Huang da W., Sherman, B. T., and Lempicki, R. A. (2009a). Bioinformatics enrichment tools: Paths toward the comprehensive functional analysis of large gene lists. *Nucleic Acids Res.* 37, 1–13. doi: 10.1093/nar/gkn923

Huang da W., Sherman, B. T., and Lempicki, R. A. (2009b). Systematic and integrative analysis of large gene lists using DAVID bioinformatics resources. *Nat. Protoc.* 4, 44–57. doi: 10.1038/nprot.2008.211

Huang, K. C., Mukhopadhyay, R., Wen, B., Gitai, Z., and Wingreen, N. S. (2008). Cell shape and cell-wall organization in Gram-negative bacteria. *Proc. Natl. Acad. Sci.* 105, 19282–19287. doi: 10.1073/pnas.0805309105

Huq, A., Colwell, R. R., Rahman, R., Ali, A., Chowdhury, M. A. R., Parveen, S., et al. (1990). Detection of *Vibrio cholerae* O1 in the aquatic environment by fluorescent-monoclonal antibody and culture methods. *Appl. Environ. Microbiol.* 56, 2370–3.

Huq, A., Small, E. B., West, P. A., Huq, M. I., Rahman, R., and Colwell, R. R. (1983). Ecological relationships between *Vibrio cholerae* and planktonic crustacean copepods. *Appl. Environ. Microbiol.* 45, 275–83.

Jenal, U., and Malone, J. (2006). Mechanisms of cyclic-di-GMP signaling in bacteria. *Annu. Rev. Genet.* 40, 385–407. doi: 10.1146/annurev.genet.40.110405.090423

Jensen, G. J., and Briegel, A. (2007). How electron cryotomography is opening a new window onto prokaryotic ultrastructure. *Curr. Opin. Struct. Biol.* 17, 260–267. doi: 10.1016/j.sbi.2007.03.002

Jonson, G., Holmgren, J., and Svennerholm, A. M. (1991). Identification of a mannose-binding pilus on *Vibrio cholerae* El Tor. *Microb. Pathog.* 11, 433–441. doi: 10.1016/0882-4010(91)90039-D

Jubair, M., Atanasova, K. R., Rahman, M., Klose, K. E., Yasmin, M., Yilmaz, O., et al. (2014). *Vibrio cholerae* persisted in microcosm for 700 days inhibits motility but promotes biofilm formation in nutrient-poor lake water microcosms. *PLoS ONE* 9:e92883. doi: 10.1371/journal.pone.0092883

Jubair, M., Morris, J. G., and Ali, A. (2012). Survival of *Vibrio cholerae* in nutrient-poor environments is associated with a novel "Persister" phenotype. *PLoS ONE* 7:e45187. doi: 10.1371/journal.pone.0045187

Kanehisa, M., Furumichi, M., Tanabe, M., Sato, Y., and Morishima, K. (2017). KEGG: new perspectives on genomes, pathways,diseases and drugs. *Nucleic Acids Res.* 45, 1–15. doi: 10.1093/nar/gkw1092

Kanehisa, M., and Goto, S. (2000). KEGG: Kyoto encyclopaedia of genes and genomes. *Nucl. Acids Res.* 28, 27–30. doi: 10.1093/nar/28.1.27

Kell, D. B., Kaprelyants, A. S., Weichart, D. H., Harwood, C. R., and Barer, M. R. (1998). Viability and activity in readily culturable bacteria: A review and discussion of the practical issues. Antonie van Leeuwenhoek. *Int. J. Gen. Mol. Microbiol.* 73, 169–187. doi: 10.1023/A:1000664013047

Kim, J. S., Chowdhury, N., Yamasaki, R., and Wood, T. K. (2018). Viable but non-culturable and persistence describe the same bacterial stress state. *Environ. Microbiol.* 20, 2038–2048. doi: 10.1111/1462-2920.14075

Kirn, T. J., Jude, B. A., and Taylor, R. K. (2005). A colonization factor links *Vibrio cholerae* environmental survival and human infection. *Nature*. 438, 863-6. doi: 10.1038/nature04249

Krachler, A. M., Ham, H., and Orth, K. (2011). Outer membrane adhesion factor multivalent adhesion molecule 7 initiates host cell binding during infection by Gram-negative pathogens. *Proc. Natl. Acad. Sci. U. S. A.* 108, 11614–11619. doi: 10.1073/pnas.1102360108

Krebs, S. J., and Taylor, R. K. (2011). Nutrient-dependent, rapid transition of *Vibrio cholerae* to coccoid morphology and expression of the toxin co-regulated pilus in this form. *Microbiology* 157, 2942–2953. doi: 10.1099/mic.0.048561-0

Kremer, J. R., Mastronarde, D. N., and McIntosh, J. R. (1996). Computer visualization of three-dimensional image data using IMOD. *J. Struct. Biol.* 116, 71–76. doi: 10.1006/jsbi.1996.0013

Lefman, J., Zhang, P., Hirai, T., Weis, R. M., Juliani, J., Bliss, D., et al. (2004). Three-dimensional electron microscopic imaging of membrane invaginations in Escherichia coli overproducing the chemotaxis receptor Tsr. *J. Bacteriol.* 186, 5052–5061. doi: 10.1128/JB.186.15.5052-5061.2004

Leighton, T. L., Dayalani, N., Sampaleanu, L. M., Howell, P. L., and Burrows, L. L. (2015). Novel role for PilNO in type IV pilus retraction revealed by alignment subcomplex mutations. *J. Bacteriol.* 197, 2229–2238. doi: 10.1128/JB.00220-15

Liu, X., Beyhan, S., Lim, B., Linington, R. G., and Yildiz, F. H. (2010). Identification and characterization of a phosphodiesterase that inversely regulates motility and biofilm formation in *Vibrio cholerae*. *J. Bacteriol.* 92, 4541-52. doi: 10.1128/JB.00209-10

May, K. L., and Silhavy, T. J. (2017). Making a membrane on the other side of the wall. *Biochim. Biophys. Acta - Mol. Cell Biol. Lipids* 1862, 1386–1393. doi: 10.1016/j.bbalip.2016.10.004

Mederma, G. J., Schets, F. M., van de Giessen, A. W., and Havelaar, A. H. (1992). Lack of colonization of 1 day old chicks by viable, non-culturable *Campylobacter jejuni*. *J. Appl. Bacteriol.* 72, 512–516. doi: 10.1111/j.1365-2672.1992.tb01868.x

Merchant, S. S., and Helmann, J. D. (2012). Elemental economy. Microbial strategies for optimizing growth in the face of nutrient limitation. *Adv. Microb. Physiol.* 60, 91–210. doi: 10.1016/B978-0-12-398264-3.00002-4

Mey, A. R., Wyckoff, E. E., Kanukurthy, V., Fisher, C. R., and Payne, S. M. (2005). Iron and Fur regulation in *Vibrio cholerae* and the role of Fur in virulence. *Infect. Immun.* 73, 8167–8178. doi: 10.1128/IAI.73.12.8167-8178.2005

Miller, C. J., Drasar, B. S., and Feachem, R. G. (1982). Cholera and estuarine salinity in Calcutta and London. *Lancet*. 319, 1216–1218. doi: 10.1016/S0140-6736(82)92340-6

Mishra, A., Taneja, N., and Sharma, M. (2012). Viability kinetics, induction, resuscitation and quantitative real-time polymerase chain reaction analyses of viable but nonculturable *Vibrio cholerae* O1 in freshwater microcosm. *J. Appl. Microbiol.* 112, 945–953. doi: 10.1111/j.1365-2672.2012.05255.x

Morishige, Y., Fujimori, K., and Amano, F. (2015). Use of Flow Cytometry for Quantitative Analysis of Metabolism of Viable but Non-culturable (VBNC) *Salmonella*. *Biol. Pharm. Bull.* 38, 1255–1264. doi: 10.1248/bpb.b15-00005

Mutreja, A., Kim, D. W., Thomson, N. R., Connor, T. R., Lee, J. H., Kariuki, S., et al. (2011). Evidence for several waves of global transmission in the seventh cholera pandemic. *Nature* 477, 462-5. doi: 10.1038/nature10392

Nelson, E. J., Chowdhury, A., Flynn, J., Schild, S., Bourassa, L., Shao, Y., et al. (2008). Transmission of *Vibrio cholerae* is antagonized by lytic phage and entry into the aquatic environment. *PLoS Pathog.* 4:e1000187. doi: 10.1371/journal.ppat.1000187

Novichkov, P. S., Kazakov, A. E., Ravcheev, D. A., Leyn, S. A., Kovaleva, G. Y., Sutormin, R. A., et al. (2013). RegPrecise 3.0 - A resource for genome-scale exploration of transcriptional regulation in bacteria. *BMC Genomics* 14:745. doi: 10.1186/1471-2164-14-745

Oikonomou, C. M., Swulius, M. T., Briegel, A., Beeby, M., Yao, Q., and Jensen, G. J. (2016). "Electron cryotomography," in *Methods in Microbiology* doi: 10.1016/bs.mim.2016.10.001

Oliver, J. D. (2005). The viable but nonculturable state in bacteria. *J. Microbiol.* 43 Spec No, 93–100.

Oliver, J. D. (2010). Recent findings on the viable but nonculturable state in pathogenic bacteria. *FEMS Microbiol. Rev.* 34, 415–425. doi: 10.1111/j.1574-6976.2009.00200.x

Oliver, J. D., Hite, F., McDougald, D., Andon, N. L., and Simpson, L. M. (1995). Entry into, and resuscitation from, the viable but nonculturable state by Vibrio vulnificus in an estuarine environment. *Appl. Environ. Microbiol.* 61, 2624–2630.

Panina, E. M., Mironov, A. A., and Gelfand, M. S. (2001). Comparative analysis of FUR regulons in gamma-proteobacteria. *Nucleic Acids Res.* 29, 5195–5206. doi: 10.1093/nar/29.24.5195

Peabody, M. A., Laird, M. R., Vlasschaert, C., Lo, R., and Brinkman, F. S. L. (2016). PSORTdb: Expanding the bacteria and archaea protein subcellular localization database to better reflect diversity in cell envelope structures. *Nucleic Acids Res.* 44, D663–D668. doi: 10.1093/nar/gkv1271

Pilhofer, M., Ladinsky, M. S., McDowall, A. W., and Jensen, G. J. (2010). Bacterial TEM. New insights from cryo-microscopy. *Methods Cell Biol.* 96, 21–45. doi: 10.1016/S0091-679X(10)96002-0

Pinto, D., Santos, M. A., and Chambel, L. (2015). Thirty years of viable but nonculturable state research: Unsolved molecular mechanisms. *Crit. Rev. Microbiol.* 41, 61–76. doi: 10.3109/1040841X.2013.794127

Pruzzo, C., Tarsi, R., Lle,ò, M. D., Signoretto, C., Zampini, M., Pane, L., et al. (2003). Persistence of adhesive properties in *Vibrio cholerae* after long-term exposure to sea water. *Environ. Microbiol.* 5, 850-8. doi: 10.1046/j.1462-2920.2003.00498.x

Rahman, I., Shahamat, M., Kirchman, P. A., Russek-Cohen, E., and Colwell, R. R. (1994). Methionine uptake and cytopathogenicity of viable but nonculturable Shigella dysenteriae type 1. *Appl. Environ. Microbiol.* 60, 3573–3578.

Sabharwal, D., Song, T., Papenfort, K., and Wai, S. N. (2015). The VrrA sRNA controls a stationary phase survival factor vrp of *Vibrio cholerae*. *RNA Biol.* 12, 186–96. doi: 10.1080/15476286.2015.1017211

Shi, J., Romero, P. R., Schoolnik, G. K., Spormann, A. M., and Karp, P. D. (2006). Evidence supporting predicted metabolic pathways for *Vibrio cholerae*: gene expression data and clinical tests. *Nucleic Acids Res.* 34, 2438–2444. doi: 10.1093/nar/gkl310

Signoretto, C., Lle,ò, M., and Canepari, P. (2002). Modification of the Peptidoglycan of Escherichia coli in the Viable But Nonculturable State. *Curr. Microbiol.* 44, 125–131. doi: 10.1007/s00284-001-0062-0

Silva, A. J., and Benitez, J. A. (2016). *Vibrio cholerae* Biofilms and cholera pathogenesis. *PLoS Negl. Trop. Dis.* doi: 10.1371/journal.pntd.0004330

Singleton, F. L., Attwell, R., Jangi, S., and Colwell, R. R. (1982a). Effects of temperature and salinity on Vibrio cholerae growth. Appl. Environ. Microbiol. 44, 1047–58.

Singleton, F. L., Attwell, R. W., Jangi, M. S., and Colwell, R. R. (1982b). Influence of salinity and organic nutrient concentration on survival and growth of *Vibrio cholerae* in aquatic microcosms. *Appl. Environ. Microbiol.* 43, 1080–1085.

Sperandio, V., Giron, J. A., Silveira, W. D., and Kaper, J. B. (1995). The OmpU outer membrane protein, a potential adherence factor of *Vibrio cholerae*. *Infect. Immun.* 63, 4433-8.

Spiro, R. G. (1966). [1] Analysis of sugars found in glycoproteins. *Methods Enzymol.* 8, 3–26. doi: 10.1016/0076-6879(66)08005-4

Syed, K. A., Beyhan, S., Correa, N., Queen, J., Liu, J., Peng, F., et al. (2009). The *Vibrio cholerae* flagellar regulatory hierarchy controls expression of virulence factors. *J. Bacteriol.* 191, 6555–6570. doi: 10.1128/JB.00949-09

Tammam, S., Sampaleanu, L. M., Koo, J., Manoharan, K., Daubaras, M., Burrows, L. L., et al. (2013). PilMNOPQ from the Pseudomonas aeruginosa type IV pilus system form a transenvelope protein interaction network that interacts with PilA. *J. Bacteriol.* 195, 2126–2135. doi: 10.1128/JB.00032-13

Tamplin, M. L., Gauzens, A. L., Huq, A., Sack, D. A., and Colwell, R. R. (1990). Attachment of Vibrio cholerae serogroup O1 to zooplankton and phytoplankton of Bangladesh waters. *Appl. Environ. Microbiol.* 56, 1977–80.

Taylor, R. K., Miller, V. L., Furlong, D. B., and Mekalanost, J. J. (1987). Use of phoA gene fusions to identify a pilus colonization factor coordinately regulated with cholera toxin. *Proc Natl Acad Sci USA.* 84, 2833–2837.

Terzieva, S., Donnelly, J., Ulevicius, V., Grinshpun, S. A., Willeke, K., Stelma, G. N., et al. (1996). Comparison of methods for detection and enumeration of airborne microorganisms collected by liquid impingement. *Appl. Environ. Microbiol.* 62, 2264–2272.

UniProt Consortium, T. (2018). UniProt: the universal protein knowledgebase. *Nucleic Acids Res.* 46, 2699–2699. doi: 10.1093/nar/gky092

Utada, A. S., Bennett, R. R., Fong, J. C. N., Gibiansky, M. L., Yildiz, F. H., Golestanian, R., et al. (2014). *Vibrio cholerae* use pili and flagella synergistically to effect motility switching and conditional surface attachment. *Nat. Commun.* 5:4913. doi: 10.1038/ncomms5913

van der Aart, L. T., Spijksma, G. K., Harms, A., Vollmer, W., Hankemeier, T., and van Wezel, G. P. (2018). High-resolution analysis of the peptidoglycan composition in *Streptomyces coelicolor*. *J. Bacteriol.* 200:e00290-18doi: 10.1128/JB.00290-18

Vital, M., Füchslin, H. P., Hammes, F., and Egli, T. (2007). Growth of *Vibrio cholerae* O1 Ogawa Eltor in freshwater. *Microbiology* 153, 1993–2001. doi: 10.1099/mic.0.2006/005173-0

Vora, G. J., Meador, C. E., Bird, M. M., Bopp, C. A., Andreadis, J. D., and Stenger, D. A. (2005). Microarray-based detection of genetic heterogeneity, antimicrobial resistance, and the viable but nonculturable state in human pathogenic Vibrio spp. *Proc. Natl. Acad. Sci. U.S.A.* 102, 19109–19114. doi: 10.1073/pnas.0505033102

Wada, A., Yamazaki, Y., Fujita, N., and Ishihama, A. (2006). Structure and probable genetic location of a "ribosome modulation factor" associated with 100S ribosomes in stationary-phase Escherichia coli cells. *Proc. Natl. Acad. Sci. U.S.A* 87, 2657–61. doi: 10.1073/pnas.87.7.2657

Xu, H. S., Roberts, N., Singleton, F. L., Attwell, R. W., Grimes, D. J., and Colwell, R. R. (1982). Survival and viability of nonculturable Escherichia coli and *Vibrio cholerae* in the estuarine and marine environment. *Microb. Ecol.* 8, 313–323. doi: 10.1007/BF02010671

Xu, T., Cao, H., Zhu, W., Wang, M., Du, Y., Yin, Z., et al. (2018). RNA-seq-based monitoring of gene expression changes of viable but non-culturable state of *Vibrio cholerae* induced by cold seawater. *Environ. Microbiol. Rep.* 10, 594–604, doi: 10.1111/1758-2229.12685

Yang, W., Alvarado, A., Glatter, T., Ringgaard, S., and Briegel, A. (2018). Baseplate variability of Vibrio choleraechemoreceptor arrays. *Proc. Natl. Acad. Sci.*, 57, 201811931. doi: 10.1073/pnas.1811931115

Zhang, P., Khursigara, C. M., Hartnell, L. M., and Subramaniam, S. (2007). Direct visualization of Escherichia coli chemotaxis receptor arrays using cryo-electron microscopy. *Proc. Natl. Acad. Sci. U S A.* 104, 3777–3781. doi: 10.1073/pnas.0610106104

Zheng, S. Q., Keszthelyi, B., Branlund, E., Lyle, J. M., Braunfeld, M. B., Sedat, J. W., et al. (2007). UCSF tomography: An integrated software suite for real-time electron microscopic tomographic data collection, alignment, and reconstruction. *J. Struct. Biol.* 157, 138–147. doi: 10.1016/j.jsb.2006.06.005

Conflict of Interest Statement: The authors declare that the research was conducted in the absence of any commercial or financial relationships that could be construed as a potential conflict of interest.